

# Hydrogel beads as slow-release $\text{NH}_4^+$ fertilizer and reducing S and Fe in soil acidity: alginate-poly(acrylic acid)-carboxymethyl cellulose-oleic acid

Endar Hidayat<sup>1\*</sup>, Nur Ain Hannani Hamid<sup>2</sup>, Nur Maisarah Mohamad Sarbani<sup>2</sup>, Muhammad Aslam Mohd Safari<sup>3</sup>, Mitsuru Aoyagi<sup>2</sup>, Hiroyuki Harada<sup>2</sup>, Sadaki Samitsu<sup>1</sup>

<sup>1</sup>Data-driven Polymer Design Group, Research Center for Macromolecules and Biomaterials, National Institute for Materials Science, 1-2-1 Sengen, Tsukuba, 305-0047, Japan

<sup>2</sup>Department of Life Systems Science, Faculty of Bioresources Science, Prefectural University of Hiroshima, Shobara 727-0023, Japan

<sup>3</sup>Department of Mathematics and Statistics, Faculty of Science, Universiti Putra Malaysia, 43400 UPM Serdang, Selangor, Malaysia

\*Corresponding author: ENDAR.Hidayat@nims.go.jp

## Abstract

A study was conducted on slow-release  $\text{NH}_4^+$  fertilizer ( $\text{SRNH}_4\text{F}$ ) embedded in a hydrogel bead matrix consisted of sodium alginate, poly(acrylic acid), and carboxymethyl cellulose, both without (SPC-A) and with (SPC-B) the incorporation of oleic acid. The results demonstrated that SPC-B exhibited higher specific surface area, pore volume and a greater abundance of  $\text{COOH}$  functional groups. Swelling behaviour analysis indicated that all samples achieved their highest swelling in  $\text{NaOH}$  solution. The  $\text{SRNH}_4\text{F}$  release studies revealed that the inclusion of oleic acid significantly reduced  $\text{NH}_4^+$  release, enabling more controlled  $\text{NH}_4^+$  ion delivery in water, while also contributing to reduced  $\text{CO}_2$  emissions from soil, consistent with the observed trends in soil organic carbon levels. Furthermore, the treatment with hydrogel beads resulted in a significant increase ( $P < 0.05$ ) in soil available phosphorus, soil cation exchange capacity, exchangeable calcium, and available ammonium nitrogen. The immobilization rates in soil were satisfactory, reaching up to 93.36% for

sulfur and 88.33% for iron with SPC-B. This technique demonstrated multifunctionality in improving nutrient management and mitigating environmental pollution.

Keywords: Hydrogel beads, sulfur and iron contamination, immobilization, oleic acid, slow release fertilizer

## 1. Introduction

In the 21st century, the agricultural sector faces significant challenges as the global population continues to surge, anticipated to surpass 9 billion by 2050 (Espécie Bueno et al., 2015). Despite the growing demand, the expansion of agricultural land is hindered by limited space, poor soil quality, and water scarcity, resulting in a decline in available farmland (Sharma et al., 2023). In response, farmers have increased fertilizer use to boost short-term crop yields per hectare (Lateef et al., 2016). Although nitrogen (N) constitutes over 80% of the atmosphere and soil, it is largely present in a non-reactive form that plants cannot directly utilize, necessitating regular supplementation through fertilizers (Sharma et al., 2023). However, plants can only absorb 30-35% of the N present in fertilizers, leading to significant energy losses because of inefficient nutrition absorption (Manto et al., 2018; Spiertz, 2010). Much of the remaining N is swiftly processed by microbes or lost through physical and chemical procedures such as leaching and volatilization (Espécie Bueno et al., 2015). N leaching contributes to the pollution of water bodies beneath the surface and poses threats to aquatic ecosystems. Consequently, the heavy use of fertilizers has led to a decline in soil quality and major environmental concerns over the long term. To address these issues and improve the efficiency of plant nutrient uptake, the introduction of a polymer-based carrier material that acts as a controlled N release system should be considered.

The utilization of polymer hydrogel to control N release represents a promising approach. The shift towards sustainable and green resources has prompted the exploration and adoption of biodegradable polymers like sodium alginate (SA), poly(acrylic acid) (PA), and carboxymethyl cellulose (CMC), which offer solutions to the cost, environmental, and manufacturing challenges associated with synthetic polymers. SA is a bio-based hydrogel known for its hydrophilic nature and non-toxicity, boasting a high capacity for swelling (Satheesh Kumar et al., 2023). However,

the stability of SA hydrogel can be compromised by the existence of certain ions or high ionic interactions. The incorporation of PA, CMC and oleic acid (OA) by cross-linking method can enhance the stability (Abd El-Aziz et al., 2022; Alam & Christopher, 2018) and mechanical strength of the hydrogel composites (Enoch & Somasundaram, 2023; Faturechi et al., 2015). This monounsaturated OA is well known for its versatility and wide range of applications in industries such as food, cosmetics, and pharmaceuticals. In recent years, studies have highlighted the remarkable role of OA in fertilizers, demonstrating its ability to stabilize particles and minimize nutrient loss (Atalay et al., 2022a). Nonetheless, when applied to soil, bulk-sized hydrogel may not distribute evenly, potentially leading to irregular water distribution around the material. In comparison, hydrogel beads, with their higher surface area to volume ratio compared to bulk hydrogels, facilitate more effective interactions with water and soil. This design enables a more uniform and controlled release of minerals, enhancing nutrient delivery and soil hydration.

Soil acidity has emerged as a critical challenge in maintaining agricultural productivity, significantly affecting food yields. The excessive use of N fertilizers is a primary factor contributing to the acidification of agricultural soils, with ammonium ( $\text{NH}_4^+$ )-based fertilizers notably increasing soil acidity (Zhang et al., 2022). In addition to  $\text{NH}_4^+$ , sulfur (S) and iron (Fe), which may originate from industrial and mining activities or from areas where pesticides are applied, can elevate levels of these elements, leading to contamination (Xu & Tsang, 2022) and acidity. During rainfall, this S and Fe can be washed into water bodies and subsequently deposit in surrounding soils. Consequently, this contamination can lead to the poisoning of clean water and food sources with S and Fe, posing serious health risks and potentially fatal impacts on human and plant life. To address this issue, the use of hydrogel bead materials has gained interest due to their effectiveness as immobilization agents for S and Fe in soils. When these elements are



immobilized, S and Fe molecules move through the hydrogel bead matrix and are captured by electrostatic interactions with hydrophilic functional groups such as hydroxyl (-OH) and carboxylate (COO<sup>-</sup>) (Li & Zhang, 2023).

Generally, soils acidity contaminated with heavy metals exhibit poor biological and physicochemical properties, including reduced organic matter, low fertility, and micronutrient imbalances, which adversely affect soil organic carbon (SOC) sequestration (Lwin et al., 2018; Ussiri & Lal, 2005). This study hypothesizes that the synergistic use of SA, PA, CMC, and OA within a hydrogel bead matrix, combined with ammonium chloride (NH<sub>4</sub>Cl) as the primary nitrogen source, can produce a material with superior water retention and contaminant-binding capabilities. This formulation is expected to be particularly effective for controlling NH<sub>4</sub><sup>+</sup> release and immobilizing S and Fe in contaminated soils. The objective of this study is to formulate a controlled-release fertilizer using hydrogel beads derived from SA, PA, CMC and OA, with NH<sub>4</sub>Cl as the primary nitrogen source. Additionally, the absence of OA was investigated to evaluate its impact on slow-release mineralization and immobilization effects. The study also examines CO<sub>2</sub> emissions during the incubation of contaminated soils to assess the environmental implications of the hydrogel formulation.

## 2. Materials and Method

### 2.1 Materials

The following chemicals were used in this study: Sulfuric acid (H<sub>2</sub>SO<sub>4</sub>, 95%), hydrochloric acid (HCl, 36.5-38%), potassium chloride (KCl, 99.5%), iron sulfate (FeSO<sub>4</sub>, >95%), sodium carbonate (Na<sub>2</sub>CO<sub>3</sub>, >99.8%), sodium bicarbonate (NaHCO<sub>3</sub>, >99.5%), sodium hydrogen phosphate (NaHPO<sub>4</sub>, >99.95%), ammonium acetate (CH<sub>3</sub>COONH<sub>4</sub>, >97%), sodium hydroxide (NaOH, 99.99%), OA (C<sub>18</sub>H<sub>34</sub>O<sub>2</sub>, 90%), and potassium dichromate (K<sub>2</sub>Cr<sub>2</sub>O<sub>7</sub>, 99.5%) were

purchased from Kanto Chemical Co. Inc., Japan. SA and PA (molecular weight: 100.000) were procured from Wako and Scientific Polymer Products, INC., New York, respectively.

## 2.2 Preparation of hydrogel beads

For the purpose to formulate hydrogel beads, 6 mL of 2 wt% SA aqueous solution, 6 mL of 5 wt% PA aqueous solution, 6 mL of 1 wt% CMC, 1 mL of 3 M NaOH, and 0.25 grams of NH<sub>4</sub>Cl for the SPC-A were combined. OA (0.05 mL) was added to SPC-B. At a constant temperature of 50 °C, the samples were agitated for 1h in bottle flasks. After cooling, the solution was gradually injected into an aqueous solution containing 10% CaCl<sub>2</sub>. To create the final hydrogel beads, the hydrogel beads were then let to grow for one night. After that, the hydrogel beads were rinsed with ethanol and deionized (DI) water and allowed to dry for 24 h at 60 °C in an oven.

## 2.3 Carboxyl groups analysis

The quantification of carboxyl groups present in the cross-linked hydrogel beads was performed via conductometric titration, as referenced in study (Yang et al., 2012). Approximately 25 mg of the dried hydrogel bead composite was combined with 2.5 mL of a 20 mM sodium chloride (NaCl) solution and stirred for 30 min to ensure even distribution throughout the mixture. HCl was added to the mixture until it reached a pH level of 3.0. To adjust the pH to 11.0, NaOH solution was added gradually to the suspension. The carboxyl group concentration within the cross-linked hydrogel beads was then calculated using Equation (3).

$$\text{COOH (mmol/g)} = \frac{V_{\text{NaOH}} \times M_{\text{NaOH}}}{W_d} \quad (3)$$

where COOH (mmol/g) denotes the concentration of carboxyl groups in the cross-linked hydrogel beads.  $V_{\text{NaOH}}$  (mL) is the volume of NaOH necessary to deprotonate the COOH groups.  $M_{\text{NaOH}}$  (mol/L) refers to the molar concentration of the NaOH solution.  $W_d$  (g) represents the mass of the hydrogel beads in their initial dry state.

## 2.4 Swelling experiments

The swelling behaviour of the hydrogel beads were conducted at 25 °C over a period of 24 h. Dried hydrogel beads were submerged in 50 mL of DI water, along with 0.01 M HCl and 0.01 M NaOH solutions, contained within a glass beaker. The percentage of swelling rate was then determined by using Equation (4).

$$\text{Swelling rate (\%)} = \frac{W_s - W_d}{W_d} \times 100 \quad (4)$$

where  $W_s$  is the weights of swollen hydrogels and  $W_d$  is the weights of dried hydrogels.

## 2.5 Determination of mineral release

Batch water shaker tests were used to measure the amounts of  $\text{NH}_4^+$  emitted from the hydrogel beads (BW101, Yamato, Japan). 50 mL of DI water, 0.01 M NaOH, 0.01 M HCl, 0.01 M NaCl, and 0.01 M  $\text{MgCl}_2$  were added to each set of beads (0.5 g), which were then shaken at 25 °C at 100 rpm. At 1, 3, 7, and 14 days intervals, the  $\text{NH}_4^+$  analysis was conducted.

## 2.6 Soil incubation contaminated S and Fe experimental design

The soil used to make artificial contaminated soil was obtained from a Shobara City market. In a plastic container, 1 kilogram of air-dried soil and 1 L of a 0.5 M  $\text{FeSO}_4$  solution were mixed together. After three days of incubation, the soil was sieved and dried for an additional three days at 60 °C. An experiment involving contaminated S and Fe was conducted over 30 days, employing two experimental conditions: one group of soil was treated with 1 wt.% SPC-A, and another with 1 wt.% SPC-B. The experiments were placed in plastic cups at room temperature. After 30 days, the soil samples were collected and oven-dried at 60 °C for three days for subsequent analysis. During the incubation, a  $\text{CO}_2$  sensor was used to measure soil  $\text{CO}_2$  emissions using the Go Direct  $\text{CO}_2$  Gas Sensor from Vernier Science Education.

## 2.7 Characterization of hydrogel beads

Nitrogen (N<sub>2</sub>) adsorption/desorption experiments was performed using temperature at 77 K a gas adsorption analyzer (BELSORP-max, MicrotracBEL, Japan). The surface areas and pore size distribution of hydrogel bead were calculated from the nitrogen adsorption isotherm based on the Brunauer-Emmett-Teller (BET) and Barrett-Joyner-Halenda (BJH) model, respectively. Thermogravimetric analysis (TGA) of hydrogel beads was carried out in an inert N<sub>2</sub> atmosphere from 50 to 800 °C at a heating rate of 60 °C min<sup>-1</sup> using a Rigaku Thermo Plus TG8120, Tokyo, Japan. A Thermo Scientific Nicolet iS10 FTIR device (Thermo Fisher Scientific Inc., Waltham, MA, USA) was used to analyze the functional groups of the hydrogel beads. Employing a benchtop SEM Miniscope TM-3000 (Hitachi-hitech, Tokyo, Japan), the structural images of the hydrogel beads were studied.

## 2.8 Determination of soil properties

The assessment of soil pH and electrical conductivity (EC) was carried out using laboratory instruments such as pH meters and EC meters. Prior to the measurement of pH and EC, a mixture was prepared with soil and water at a 1:5 (w/v) ratio and stirred for 30 min. The available phosphorus (P) content in the soil was identified using the Olsen method, which involves a 0.5 M NaHCO<sub>3</sub> solution. The exchangeable cations, specifically calcium (Ca), potassium (K), and magnesium (Mg), were evaluated using an CH<sub>3</sub>COONH<sub>4</sub> extraction method at a normality of 1 N. Additionally, to ascertain the soil's cation exchange capacity (CEC), 10 wt% sodium chloride (NaCl) was integrated with the soil. For the extraction of soil-available nitrogen-ammonium (N-NH<sub>4</sub>) and nitrogen-nitrate (N-NO<sub>3</sub>), a 2 M KCl solution was utilized. SOC levels were evaluated utilizing the Walkley-Black wet oxidation technique and the subsequent measurements were conducted by employing a UV-Visible Spectrophotometer (JASCO V-530) at a wavelength of 561

nm. To evaluate the levels of available S and Fe, the soil underwent treatment with a 20 mM solution of CaCl<sub>2</sub> at a 1:5 w/v ratio for a period of 30 min. The quantification of S was analysed using BaCl<sub>2</sub>-tween 80 solution utilizing a UV-Visible Spectrophotometer (JASCO V-530) at a wavelength of 432 nm. While Fe amount was then performed using pack testing methods at Kyoritsu Chemical-Check Lab., Corp. in Kanagawa, Japan. Bulk density (Equation 5) and soil porosity (Equation 6) were measured using below equation.

$$\rho \text{ (g/cm}^3\text{)} = \left( \frac{\text{Mass of dry soil}}{\text{Volume of dry soil}} \right) \times 100 \quad (5)$$

$$\phi \text{ (\%)} = \left( 1 - \frac{\rho}{\rho_p} \right) \times 100 \quad (6)$$

where,  $\rho$  is the bulk density,  $\rho_p$  is the soil particle density can be assumed to be 2.65 g/cm<sup>3</sup>,  $\phi$  is the soil porosity.

## 2.9 Statistical analysis

Data analyses were carried out with MINITAB software (version 21.3.1). One-way analysis of variance (ANOVA) was performed on mean data, and Tukey's test (P-value <0.05) was applied to compare treatments.

## 3. Results and discussion

### 3.1 Characteristics of hydrogel beads

Fig. 1 illustrates the SEM morphology images of dried hydrogel beads. These images show that both SPC-A and SPC-B possess a 3D interconnected porous structure with macro- and micropores. In comparison to SPC-B, SPC-A has a rougher, less uniform surface with more open pores before being incubated (Fig. 1(a) and 1(b)). Due to the absence of OA, these inconsistencies suggest a less compact structure. Recent studies (Enoch & Somasundaram, 2023) reported that hydrogels without hydrophobic additives such as OA typically have more irregular pores and

rougher surfaces. In contrast, SPC-B exhibits a more homogeneous, compact shape with fewer open pores (Fig. 1(c) and 1(d)). This homogeneity is probably the result of OA stabilizing the polymer network and increasing crosslinking density. It has been demonstrated that the addition of hydrophobic substances, like OA, decreases surface porosity and produces a more cohesive network of polymers (Atalay et al., 2022b). Following incubation, SPC-A maintains its rough, uneven shape, with minor pore structural alterations most likely caused by soil interactions (Fig. 1(e) and 1(f)). S and Fe may become immobilized more easily due to the open pores. Through their improved diffusion channels, hydrogels with more porous structures are excellent at adsorbing pollutants from soil (Lwin et al., 2018). Post incubation, SPC-B exhibits very slight alterations in surface morphology and pore size, remaining comparatively stable (Fig. 1(g) and 1(h)). OA's hydrophobic and compact properties may support the structural integrity. Major morphological modifications during environmental interactions are resisted by stable hydrogels with improved crosslinking and decreased porosity (Abd El-Aziz et al., 2022; Li & Zhang, 2023).

Fig. 2a and 2b show the N<sub>2</sub> adsorption/desorption and pore size distribution, respectively, and Table 1 summarizes the BET-specific surface area ( $S_{\text{BET}}$ ), total pore volume ( $V_{\text{total}}$ ), and the amount of COOH groups in the hydrogel beads. The data reveal that SPC-B exhibits the highest  $S_{\text{BET}}$ , with a value of 14.922 m<sup>2</sup> g<sup>-1</sup>, whereas SPC-A with 11.313, showing a 24.28% difference due to the introduction of OA. Similarly, the  $V_{\text{total}}$  and number of COOH groups in SPC-B is higher than in SPC-A, with 38.27% and 44.64% difference, respectively. This difference could be attributed to the reaction of OA with other functional groups in the hydrogel beads, possibly forming cross-links that stabilize the hydrogel structure. This stabilization likely prevents the loss or transformation of COOH groups during bead preparation and washing, thereby increasing the number of COOH groups, enhancing surface area and pore volume.

The adsorption spectra of functional groups in the hydrogel beads are depicted in Fig. 2c. The spectral range from 3008  $\text{cm}^{-1}$  to 3524  $\text{cm}^{-1}$  is assigned as the stretching vibrations of O–H bonds. A new appearance peak for SPC-B at 2161  $\text{cm}^{-1}$  is characteristics of  $\text{C}\equiv\text{C}$  (Ashby et al., 2014), might be due to the presence of OA in the hydrogel bead composite. Distinct sharp peak intensities found at 1544  $\text{cm}^{-1}$  and 1547  $\text{cm}^{-1}$  for SPC-A and SPC-B, respectively, particularly associated with the carboxylate ( $-\text{COO}^-$ ) groups (Hua et al., 2010). The peaks around 1417  $\text{cm}^{-1}$ , 1328  $\text{cm}^{-1}$  and 1083  $\text{cm}^{-1}$  can be attributed to the symmetric stretching of carboxylate ( $-\text{COO}^-$ ), (C–O), and (C–O–C), respectively (Hua et al., 2010). Additionally, the peak at 594  $\text{cm}^{-1}$  suggests the presence of the stretching vibration of the Ca–O bond.

Thermal stability analysis is a crucial step in evaluating the capabilities and limitations of hydrogel beads for their final application in the field. The TGA curves of the hydrogel beads are presented in Fig. 2d. The data show that the initial temperature of polymeric decomposition occurs at 160 °C (with a 29% weight loss) for SPC-A and 165 °C (with a 22% weight loss) for SPC-B. At the end of the analysis (800 °C), the residue remaining for SPC-A and SPC-B was 48% and 58%, respectively. These results suggest that the incorporation of OA enhances the thermal stability of the hydrogel beads.

### 3.2 $\text{NH}_4^+$ release rate

This current study evaluated the  $\text{NH}_4^+$  release profiles of hydrogel bead composites using DI water, NaOH and HCl. As shown in the results, SPC-A dissolves more readily than SPC-B, which results in a higher  $\text{NH}_4^+$  release (Fig. 2e). The mean release rates of SPC-A were 12.59 mg/L, 11.78 mg/L, and 14.73 mg/L for DI water, NaOH, and HCl, respectively, whereas for SPC-B, they were 9.39 mg/L, 9.08 mg/L, and 10.05 mg/L. This suggests a distinction of approximately 25.45%, 22.91%, and 31.77% in  $\text{NH}_4^+$  release. These percentage variations could be attributed to the layers

of OA's complex and intricate structure, which prevents minerals from moving freely across the polymer network and into the environment around them. These differences also may propose the function of OA as binding agent to facilitate a more controlled nutrient release system and prevent the loss of nutrients. The possible mechanisms of slow  $\text{NH}_4^+$  ion release from hydrogel matrix as shown in Fig. 3a.

### 3.2 Swelling behaviour

Fig. 3b illustrates the swelling behaviour of hydrogel beads when exposed to DI water, NaOH, HCl, NaCl and  $\text{MgCl}_2$  solutions. The findings revealed that the swelling rate under NaOH solution achieved higher result for both samples compared to others solution. This suggests that the hydrogel beads possess ionizable functionalities, such as carboxylic acid ( $-\text{COOH}$ ) or its deprotonated form, carboxylate ( $-\text{COO}^-$ ). In neutral, acidic, and salt conditions, these groups tend to remain protonated ( $\text{COOH}$ ), fostering strong electrostatic forces within the hydrogel matrix. Such forces could hinder the hydrogel's capacity to absorb water, thereby constraining its swelling capability (Al-qudah et al., 2014). SPC-A possess greater result for water retention compared to SPC-B. This might be due to the oleate ions, which are more hydrophobic compared to the non-ionized form of OA, indicating a lower affinity toward water molecules.

### 3.4 Impacts of amendments on soil $\text{CO}_2$ emissions

Effect of hydrogel beads on carbon dioxide emission rate is presented in Fig. 3c. Carbon dioxide emission results were significant at all the studied durations. Maximum carbon dioxide emissions (869 mg/L for intact soil (control), 714 mg/L for SPC-A and 583 mg/L for SPC-B) was found at 9 days after incubation, then it decreased and increased with the increase of time. However, SPC-B showed the lowest value compared to the SPC-A and control, which indicates that the



presence of oleate ions in hydrogel bead composite might have capability to hold or sequester CO<sub>2</sub> emission from soil.

### 3.5 Soil properties

The SEM micrographs of soil samples after the application of hydrogel beads are shown in Fig. 4a-c. The images reveal that the soil structure treated with hydrogel beads contains particles with visible pores, making it less dense and compact compared to untreated soil samples. Additionally, unlike the untreated soil, the soil aggregates treated with hydrogel beads display porous spaces, which contribute to a reduction in the soil's bulk density. Table 2 shows the soil's bulk density and porosity after a 30-day incubation period. The data suggest that adding hydrogel beads to the soil reduces its bulk density. This decrease is likely due to the hydrogel beads absorbing water and swelling, which increases their volume. As a result, the swollen beads displace soil particles, increasing the total soil volume without a proportional increase in mass, thereby lowering the bulk density. Furthermore, the porosity of the soil increased with incorporating hydrogel beads. The beads encourage the formation of soil aggregates and clusters of particles, creating larger pore spaces between them and improving the overall porosity of the soil.

### 3.5 Impacts of amendments on soil characteristics

Fig. 5 depicts the impact of treatment amendments on soil pH, EC, available P, CEC, SOC, available S, available Fe and immobilization rate of S and Fe under high contaminated S and Fe. As shown in Fig. 5a and 5b, the soil pH and EC showed no significant difference for all samples. Conversely, the level of available phosphorus (P) in the soil showed a relevant increase ( $P < 0.05$ ) following treatment with the order of increase being SPC-B > SPC-A > soil, as illustrated in Fig. 5c. This enhancement in available P may be attributed that oleate ion promotes to the mineralization of P during the incubation period. Furthermore, the cation CEC of the soil was significantly

enhanced ( $P<0.05$ ) when examined to the soil (control) (Fig. 5d). This increase is likely due the presence of  $-OH$  and  $-COOH$  groups from polymer materials in hydrogel beads. Fig. 5e-h displayed the exchangeable cations for Mg, Ca, K and Na. The results show that there are no significant differences for Mg and K, by contrast to the Ca and Na values ( $P<0.05$ ). This possibly could be due to the existence of Ca from hydrogel beads which enhances the soil Ca, whereas Na ions were adsorb into the hydrogel beads leading to a decreased in Na value in soil.

Fig. 6a-b show the available  $N-NH_4$  and  $N-NO_3$  levels in the soil. The result shows that there is a significant difference for  $N-NH_4$  value, in contrast to  $N-NO_3$ . Moreover, SPC-B applications show the highest  $N-NH_4$  and lowest the content of  $N-NO_3$ . This might be due to the presence of oleate ion that prevents  $N-NH_4$  from being oxidized and turning into  $N-NO_3$ . Fig. 6c show the concentration of available S in soil decreased markedly following the application of treated hydrogel beads ( $P<0.05$ ). After 30-day incubation period, the S concentrations were reduced to 3514 mg/Kg and 450 mg/Kg for SPC-A and SPC-B, respectively, from 6770 mg/Kg (intact soil, control). This corresponds to immobilization rates of 48.10% for SPC-A and 93.36% for SPC-B. Similarly, the Fe concentrations were also reduced with immobilization rates of 87.03% for SPC-A and 88.33% for SPC-B (Fig. 6d). Moreover, the SOC value showed significant changes ( $P<0.05$ ) with the addition of hydrogel bead amendments following treatment SPC-B>SPC-A>soil, as displayed in Fig. 6e. This might be due to the oleate ion interaction with soil minerals and organic matter to form more stable organo-mineral complexes. These complexes can protect organic carbon from rapid decomposition, thereby increasing the SOC. This finding might suggest a correlation between SOC and  $CO_2$  emission (Fig. 6f) which contributes long-term carbon sequestration in the soil.

#### 4. Conclusions

The present experiment explored and investigation of slow-release  $\text{NH}_4^+$  fertilizer embedded in hydrogel bead matrix from SA, PA, carboxymethyl cellulose in the absence (SPC-A) and presence (SPC-B) of OA. The results show that SPC-B has specific surface area, pore volume and the amount of COOH groups. Swelling behaviour indicates that the highest results was obtained under NaOH solution for all samples. Slow-release fertilizer studies showed that the presence of OA has lower release of  $\text{NH}_4^+$ , allowing for a more controlled release of nutrient, with difference percentage of 25.45%, 22.91%, and 31.77%, for DI water, NaOH and HCl, respectively. The soil incubation experiments show that the presence of OA in hydrogel bead matrix has capability to sequester  $\text{CO}_2$  emission from soil, which aligned with the trend results of SOC. Additionally, a significant increase for soil available P, CEC, exchangeable Ca and available N- $\text{NH}_4$  ( $P < 0.05$ ) after treated hydrogel bead. The immobilization rate shows satisfactory up to 93.36% for S and 88.33% for Fe, indicating effective retention of these elements in the system.

## 5. Acknowledgement

The author (E.H) would like to thank Japan Society for the Promotion of Science (JSPS) Postdoctoral Fellowship for funding this study.

## References

- Abd El-Aziz, M. E., Salama, D. M., Morsi, S. M. M., Youssef, A. M., & El-Sakhawy, M. (2022). Development of polymer composites and encapsulation technology for slow-release fertilizers. *Reviews in Chemical Engineering*, 38(5), 603–616. <https://doi.org/10.1515/revce-2020-0044>
- Alam, M. N., & Christopher, L. P. (2018). Natural Cellulose-Chitosan Cross-Linked Superabsorbent Hydrogels with Superior Swelling Properties. *ACS Sustainable Chemistry & Engineering*, 6(7), 8736–8742. <https://doi.org/10.1021/acssuschemeng.8b01062>

- Al-qudah, Y. H. F., Mahmoud, G. A., & Abdel Khalek, M. A. (2014). Radiation crosslinked poly (vinyl alcohol)/acrylic acid copolymer for removal of heavy metal ions from aqueous solutions. *Journal of Radiation Research and Applied Sciences*, 7(2), 135–145. <https://doi.org/10.1016/j.jrras.2013.12.008>
- Ashby, S. P., Thomas, J. A., García-Cañadas, J., Min, G., Corps, J., Powell, A. V., Xu, H., Shen, W., & Chao, Y. (2014). Bridging silicon nanoparticles and thermoelectrics: phenylacetylene functionalization. *Faraday Discuss.*, 176, 349–361. <https://doi.org/10.1039/C4FD00109E>
- Atalay, S., Sargin, I., & Arslan, G. (2022a). Slow-release mineral fertilizer system with chitosan and oleic acid-coated struvite-K derived from pumpkin pulp. *Cellulose*, 29(4), 2513–2523. <https://doi.org/10.1007/s10570-022-04453-5>
- Atalay, S., Sargin, I., & Arslan, G. (2022b). Slow-release mineral fertilizer system with chitosan and oleic acid-coated struvite-K derived from pumpkin pulp. *Cellulose*, 29(4), 2513–2523. <https://doi.org/10.1007/s10570-022-04453-5>
- Enoch, K., & Somasundaram, A. A. (2023). Rheological insights on Carboxymethyl cellulose hydrogels. *International Journal of Biological Macromolecules*, 253, 127481. <https://doi.org/10.1016/j.ijbiomac.2023.127481>
- Espécie Bueno, S. C., Filho, M. B., de Almeida, P. S. G., Polidoro, J. C., Olivares, F. L., Sthel, M. S., Vargas, H., Mota, L., & da Silva, M. G. (2015). Cuban zeolite as ammonium carrier in urea-based fertilizer pellets: Photoacoustic-based sensor for monitoring N-ammonia losses by volatilization in aqueous solutions. *Sensors and Actuators B: Chemical*, 212, 35–40. <https://doi.org/10.1016/j.snb.2015.01.114>

366 Faturechi, R., Karimi, A., Hashemi, A., Yousefi, H., & Navidbakhsh, M. (2015). Influence of  
 367 Poly(acrylic acid) on the mechanical properties of composite hydrogels. *Advances in Polymer*  
 368 *Technology*, 34(2). <https://doi.org/10.1002/adv.21487>  
 369 Hua, S., Ma, H., Li, X., Yang, H., & Wang, A. (2010). pH-sensitive sodium alginate/poly(vinyl  
 370 alcohol) hydrogel beads prepared by combined Ca<sup>2+</sup> crosslinking and freeze-thawing cycles  
 371 for controlled release of diclofenac sodium. *International Journal of Biological*  
 372 *Macromolecules*, 46(5), 517–523. <https://doi.org/10.1016/j.ijbiomac.2010.03.004>  
 373 Lateef, A., Nazir, R., Jamil, N., Alam, S., Shah, R., Khan, M. N., & Saleem, M. (2016). Synthesis  
 374 and characterization of zeolite based nano-composite: An environment friendly slow release  
 375 fertilizer. *Microporous and Mesoporous Materials*, 232, 174–183.  
 376 <https://doi.org/10.1016/j.micromeso.2016.06.020>  
 377 Li, Z., & Zhang, M. (2023). Progress in the Preparation of Stimulus-Responsive Cellulose  
 378 Hydrogels and Their Application in Slow-Release Fertilizers. *Polymers*, 15(17), 3643.  
 379 <https://doi.org/10.3390/polym15173643>  
 380 Lwin, C. S., Seo, B.-H., Kim, H.-U., Owens, G., & Kim, K.-R. (2018). Application of soil  
 381 amendments to contaminated soils for heavy metal immobilization and improved soil  
 382 quality—a critical review. *Soil Science and Plant Nutrition*, 64(2), 156–167.  
 383 <https://doi.org/10.1080/00380768.2018.1440938>  
 384 Manto, M. J., Xie, P., Keller, M. A., Liano, W. E., Pu, T., & Wang, C. (2018). Recovery of  
 385 ammonium from aqueous solutions using ZSM-5. *Chemosphere*, 198, 501–509.  
 386 <https://doi.org/10.1016/j.chemosphere.2018.01.126>  
 387 Satheesh Kumar, K. V., Bindu, M., Suresh, S., Anil, A., Sujoy, S., Mohanan, A., & Periyat, P.  
 388 (2023). Investigation on swelling behavior of sodium alginate/black titania nanocomposite

hydrogels and effect of synthesis conditions on water uptake. *Results in Engineering*, 20, 101460. <https://doi.org/10.1016/j.rineng.2023.101460>

Sharma, N., Allardyce, B. J., Rajkhowa, R., & Agrawal, R. (2023). Controlled release fertilizer delivery system derived from rice straw cellulose nanofibres: a circular economy based solution for sustainable development. *Bioengineered*, 14(1). <https://doi.org/10.1080/21655979.2023.2242124>

Sornkamnerd, S., Okajima, M. K., & Kaneko, T. (2017). Tough and Porous Hydrogels Prepared by Simple Lyophilization of LC Gels. *ACS Omega*, 2(8), 5304–5314. <https://doi.org/10.1021/acsomega.7b00602>

Spiertz, J. H. J. (2010). Nitrogen, sustainable agriculture and food security. A review. *Agronomy for Sustainable Development*, 30(1), 43–55. <https://doi.org/10.1051/agro:2008064>

Ussiri, D. A. N., & Lal, R. (2005). Carbon Sequestration in Reclaimed Minesoils. *Critical Reviews in Plant Sciences*, 24(3), 151–165. <https://doi.org/10.1080/07352680591002147>

Xu, Z., & Tsang, D. C. W. (2022). Redox-induced transformation of potentially toxic elements with organic carbon in soil. *Carbon Research*, 1(1), 9. <https://doi.org/10.1007/s44246-022-00010-8>

Yang, H., Tejado, A., Alam, N., Antal, M., & van de Ven, T. G. M. (2012). Films Prepared from Electrosterically Stabilized Nanocrystalline Cellulose. *Langmuir*, 28(20), 7834–7842. <https://doi.org/10.1021/la2049663>

Zhang, Y., Ye, C., Su, Y., Peng, W., Lu, R., Liu, Y., Huang, H., He, X., Yang, M., & Zhu, S. (2022). Soil Acidification caused by excessive application of nitrogen fertilizer aggravates soil-borne diseases: Evidence from literature review and field trials. *Agriculture, Ecosystems & Environment*, 340, 108176. <https://doi.org/10.1016/j.agee.2022.108176>

412

413

414

415

416

417

418

419

420

421

422

423

424

425

426

427

428

429

430

431

432

433

434

435

436

437

438

439

440

441

442

443

444

445

446

447

448

449

450

451

452

453

454

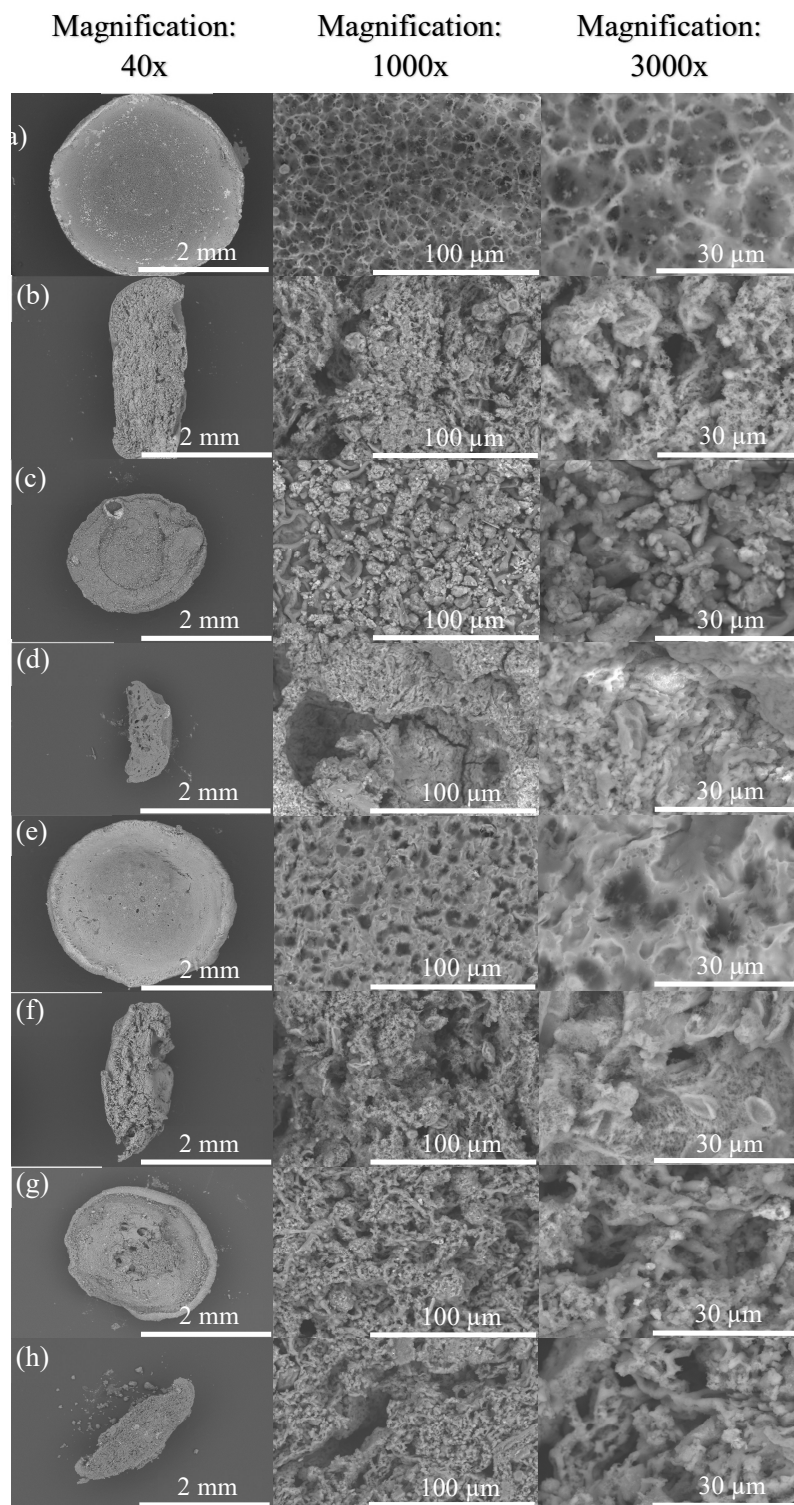


Figure 1. SEM photograph of hydrogel beads (a) SPC-A before incubation, (b) Cross-section of SPC-A before incubation, (c) SPC-B before incubation, (d) Cross-section of SPC-B before incubation, (e) SPC-A after incubation, (f) Cross-section of SPC-A after incubation, (g) SPC-B after incubation, (h) Cross-section of SPC-B after incubation.



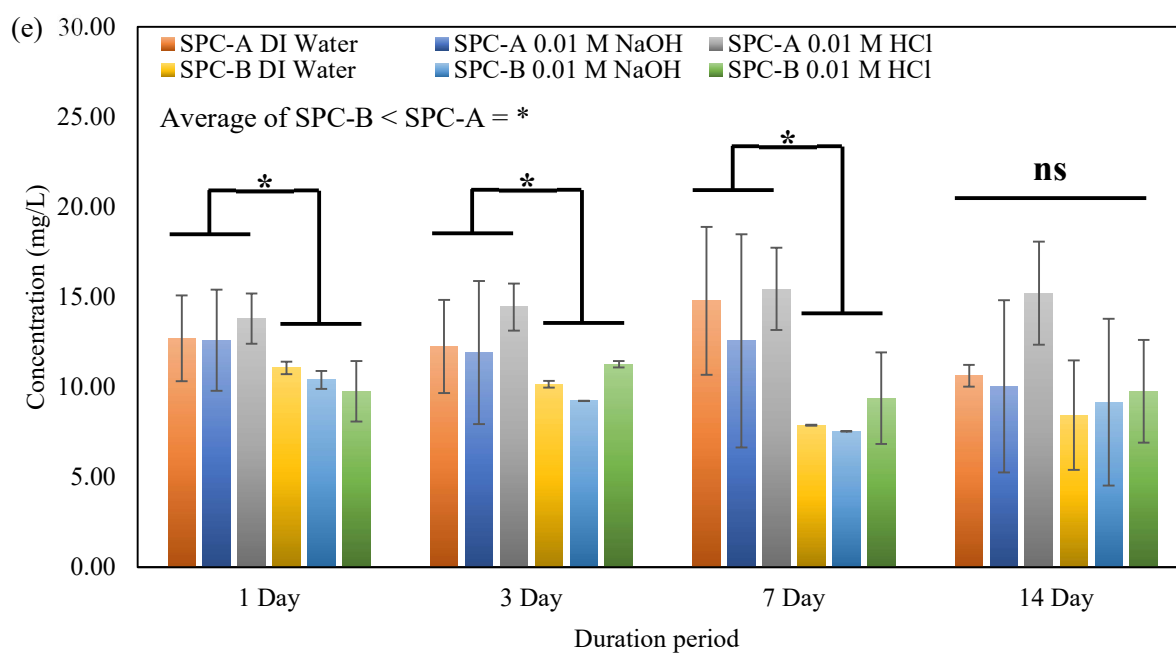
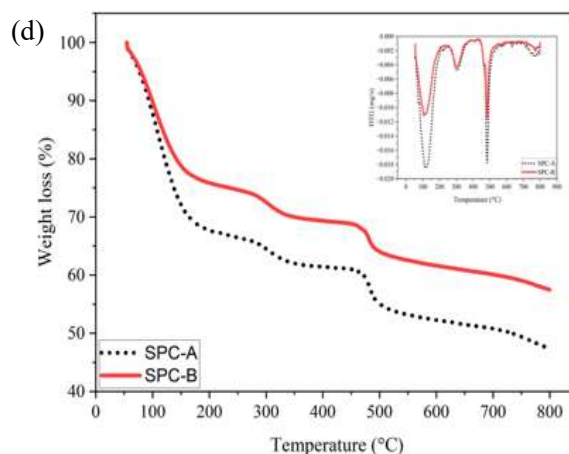
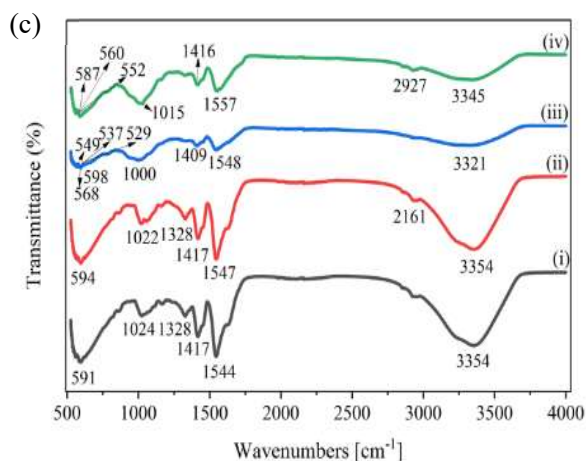
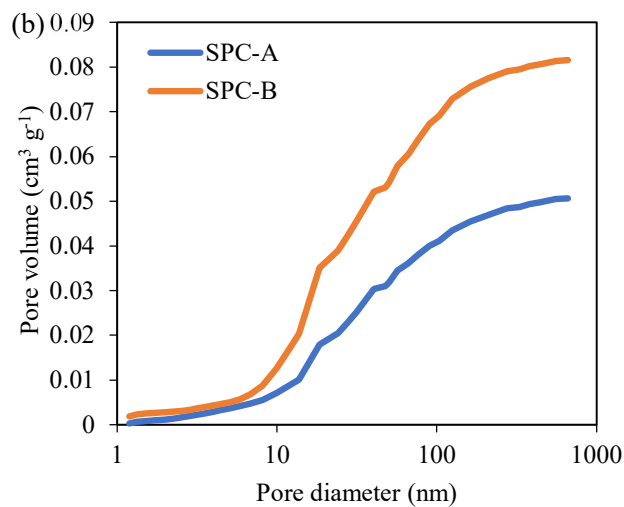
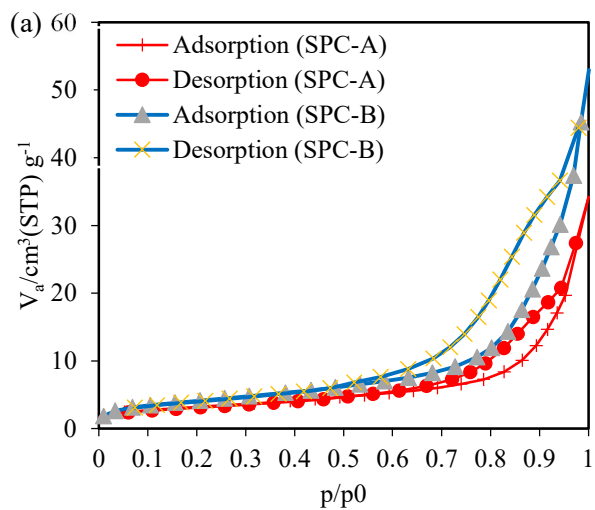


Figure 2. (a) N<sub>2</sub> isotherm adsorption/desorption (b) BJH pore size distribution (c) FTIR spectra of hydrogel beads (i: SPC-A before incubation, ii: SPC-B before incubation, iii: SPC-A after incubation, iv: SPC-B after incubation), (d) TGA of hydrogel beads before incubation, (e) slow release NH<sub>4</sub><sup>+</sup> rate from hydrogel beads. (\*) Indicates statistically significant at a significance level of  $P \leq 0.05$ ; (ns) denotes no significant difference in Tukey's test,

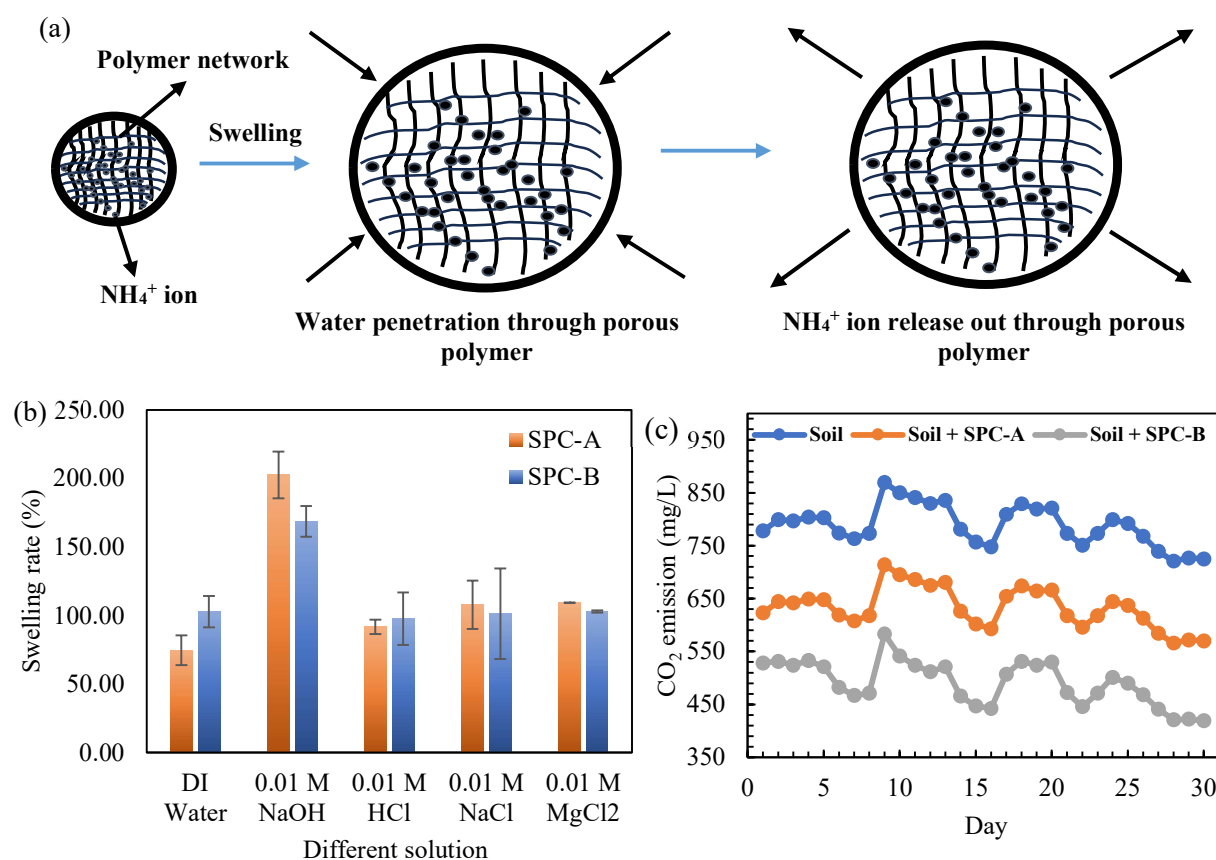


Figure 3. (a) possible mechanisms of  $\text{NH}_4^+$  ion release through polymer matrix (b) swelling behaviour of hydrogel beads before incubation, and (c)  $\text{CO}_2$  emission from soil regarding hydrogel beads application.

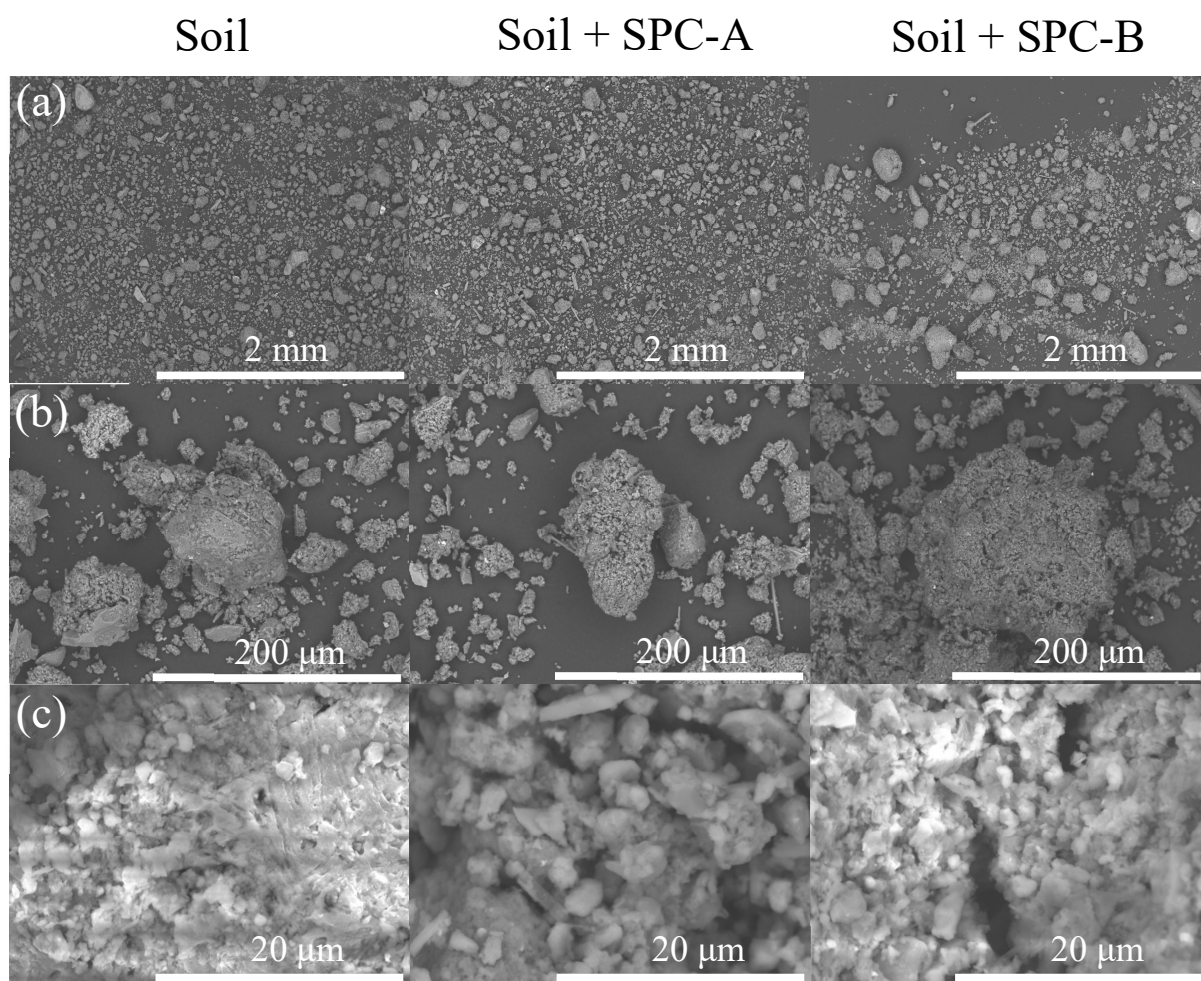


Figure 4. SEM images (a) magnification 50x, (b) magnification 500x, (c) magnification 5000x.

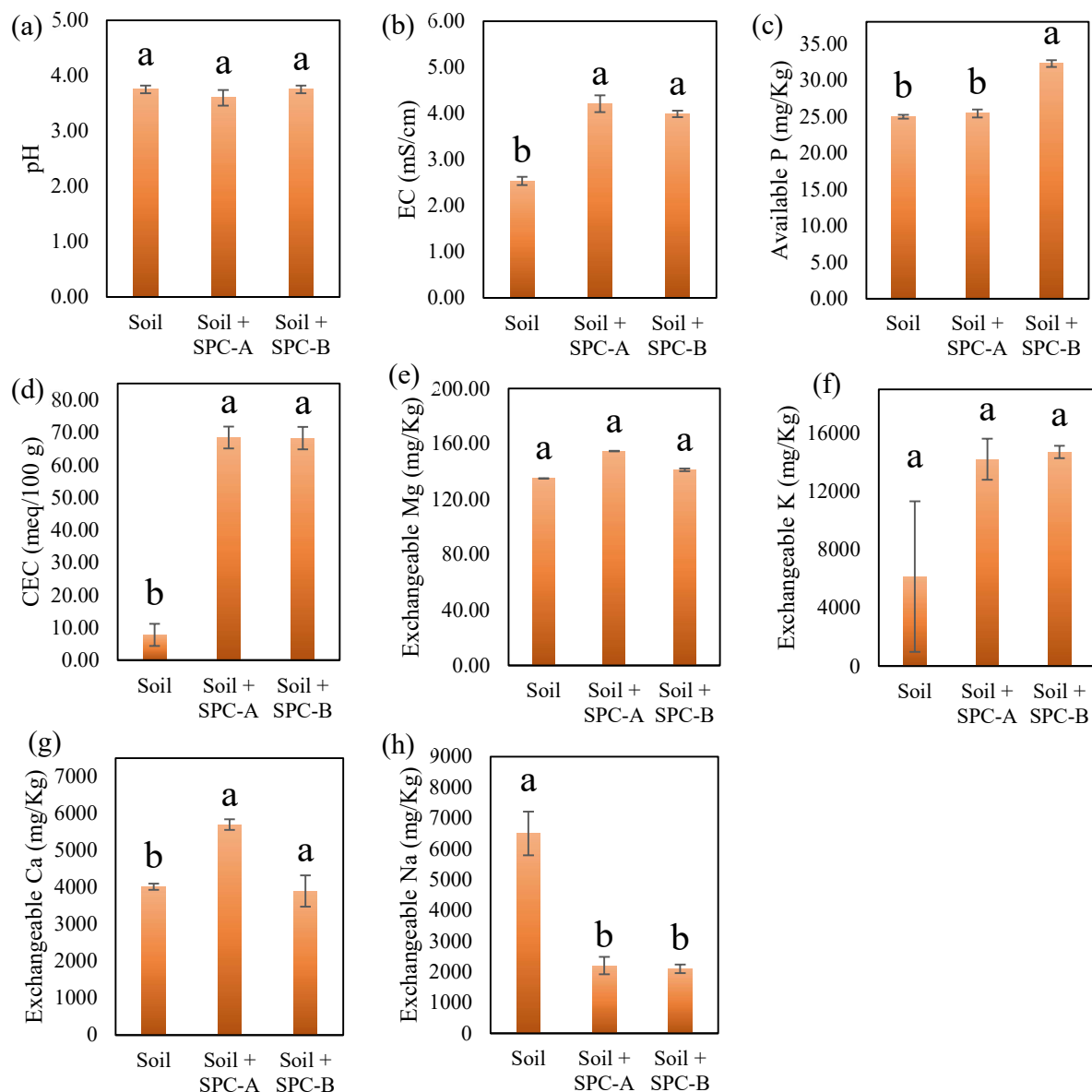


Figure 5. Effect of hydrogel beads on soil characteristics after 30 days of incubation. (a) pH, (b) electrical conductivity, (c) available P, (d) cation exchange capacity, (e) exchangeable Mg, (f) exchangeable K, (g) exchangeable Ca, and (h) exchangeable Na. Statistically significant at a significance level of  $P \leq 0.05$  in Tukey's test.

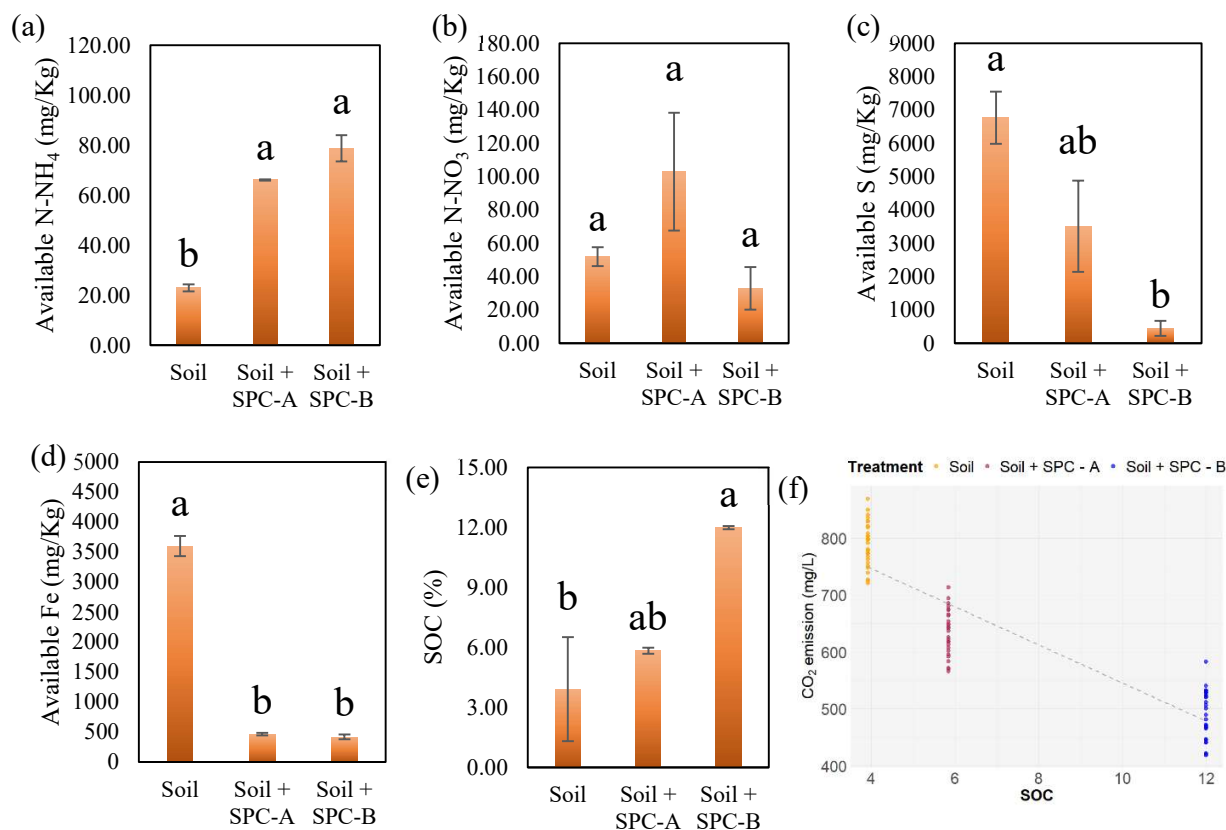


Figure 6. Effect of hydrogel beads on soil characteristics after 30 days of incubation. (a) available N-NH<sub>4</sub>, (b) available N-NO<sub>3</sub>, (c) available S, (d) available Fe, (e) SOC, and (f) Linear correlation between soil CO<sub>2</sub> and SOC (R<sup>2</sup>=1). Statistically significant at a significance level of  $P \leq 0.05$  in Tukey's test.

616 Table 1. Characteristics of hydrogel bead.

Samples	$S_{\text{BET}}$ [ $\text{m}^2 \text{g}^{-1}$ ]	$V_{\text{total}}$ [ $\text{cm}^3 \text{g}^{-1}$ ]	COOH [mmol/g]
SPC-A	11.313	0.050	$21.33 \pm 5.83$
SPC-B	14.922	0.081	$38.53 \pm 10.04$

617  
618

619 Table 2. Soil physical characteristics after 30 days of incubation.

Samples	$\rho$ ( $\text{g}/\text{cm}^3$ )	$\phi$ (%)
Soil	$0.86 \pm 0.04$	$67.56 \pm 1.55$
Soil + SPC-A	$0.84 \pm 0.03$	$68.37 \pm 1.04$
Soil + SPC-B	$0.83 \pm 0.08$	$68.79 \pm 3.00$

620